Biological Conservation 227 (2018) 352–360

Contents lists available at ScienceDirect

Biological Conservation

journal homepage: www.elsevier.com/locate/biocon

Direct modelling of limited migration improves projected distributions of Himalayan amphibians under climate change

Barkha Subba[a,b,*], Sandeep Sen[a,b], Gudasalamani Ravikanth[a], Michael Peter Nobis[c]

[a] Suri Sehgal Centre for Biodiversity and Conservation, Ashoka Trust for Research in Ecology and the Environment (ATREE), Royal Enclave, Sriramapura, Jakkur PO, Bangalore, Karnataka 560064, India
[b] Manipal Academy of Higher Education, Manipal, Karnataka 576504. India
[c] Swiss Federal Research Institute WSL, Zürcherstrasse 111, CH-8903 Birmensdorf, Switzerland

ARTICLE INFO

Keywords:
Amphibian distributions
Climate change
Eastern Himalaya
High elevation
KISSMig
MaxEnt
Migration rates

ABSTRACT

Amphibians are one of the most vulnerable taxa at risk of rapid decline under climate change. Here, we evaluated the impact of different migration constraints on projected future distributions of four high elevation frogs, belonging to the genus *Scutiger*, in the Eastern Himalaya. We explored differences between the output of conventional models assuming no or unlimited migration versus models considering plausible migration rates to ascertain future species distributions under climate change. Distributions of the four *Scutiger* species, namely *S. boulengeri*, *S. glandulatus*, *S. sikimmesis* and *S. tuberculatus*, based on field data and other sources were modelled using MaxEnt and projected for three future time periods (2021–2040; 2041–2060; 2061–2080) under the relatively ambitious RCP4.5 and the more pessimistic RCP8.5 climate change scenarios using three global circulation models. Projected species distributions were compared at different spatial resolutions (1 km, 5 km and 10 km) and for five assumptions about species migration: (1) no migration; (2–4) low, medium and high migration abilities using the KISSMig model; and (5) unlimited migration. Without migration, the projected future distribution of all four species showed a significant decrease of −15% to −64% by 2080. In contrast, three out of the four study species were projected to expand their distribution under unlimited migration scenarios. Models with more realistic migration rates, however, demonstrated considerable deviance from both no migration and unlimited migration scenarios. These results were consistent across models with different spatial resolutions. Our study shows that ignoring realistic migration constraints can lead to ineffective conservation measures by overestimating the future distribution of Himalayan amphibians. The proposed framework can be used to project more realistic ranges of future species distributions by considering the accessibility of future suitable areas, a key factor for species persistence under climate change.

1. Introduction

Global climate change is a major threat to biodiversity in many ecosystem types and is one of the main drivers in brewing a 'perfect storm' for the sixth mass extinction (Barnosky et al., 2011). There has been a remarkable increase in the global average temperature, by 0.85 °C from 1880 to 2012 (IPCC, 2013). By the end of this century it is expected to rise further, by a minimum of 0.3 °C to 1.7 °C and by a maximum of 2.6 °C to 4.8 °C (IPCC, 2013). Climate change is expected to cause the greatest change in biodiversity in high latitude/elevation ecosystems (Sala et al., 2000) and may surpass habitat loss as the primary threat to global biodiversity over the next decades (Leadley, 2010).

The Himalayan mountain chains are one of the largest geomorphological features of the world. They include three biodiversity hotspots and are home to a remarkably large number of species, including > 10,000 species of plants, 300 mammals, 977 birds, 176 reptiles and 105 amphibians, many of which are endemic (WWF, 2015). Temperature in the Himalaya is rising at twice the average rate of warming in the northern hemisphere (F. Chen et al., 2009). As a result, species in the Himalaya tend to undergo range shifts (Li et al., 2016), range expansion (Shrestha and Bawa, 2014) or range contraction (Telwala et al., 2013). The existence of large patches of climate refugia in the Himalaya sheltered its biodiversity during past glacial–interglacial cycles (Li et al., 2011). However, under the current combination of accelerating global warming and habitat fragmentation, many

* Corresponding author at: Suri Sehgal Centre for Biodiversity and Conservation, Ashoka Trust for Research in Ecology and the Environment (ATREE), Royal Enclave, Sriramapura, Jakkur PO, Bangalore, Karnataka 560064, India.
E-mail addresses: barkha.subba@atree.org (B. Subba), sandeep.sen@atree.org (S. Sen), gravikanth@atree.org (G. Ravikanth), michael.nobis@wsl.ch (M.P. Nobis).

https://doi.org/10.1016/j.biocon.2018.09.035
Received 31 May 2018; Received in revised form 20 September 2018; Accepted 30 September 2018
Available online 06 October 2018
0006-3207/

Himalayan species probably will not be able to keep pace with and adapt to the changing climate (Xu et al., 2009).

Amphibians belong to the most vulnerable taxa because of their low dispersal ability in the face of rapid ongoing climate change (Lawler et al., 2009; Warren et al., 2013) and they are rapidly declining worldwide (Bishop et al., 2012; Yiming and Cohen, 2013), with 41% of the described species falling under the threatened category (IUCN, 2016; Leung et al., 2017). Warren et al. (2013) suggested that without proper mitigation strategies about half of the amphibian species will lose more than half of their climatic range by the 2080s. A recent review of climate change research on amphibians and reptiles concluded that there is a severe geographical bias in the study of climate change effects on herpetofauna, with the highest percentage (70%) of publications coming from Europe and North America and the lowest percentage (5%) from Asia (Winter et al., 2016). Further, the authors reported a lack of studies related to climate change effects on herpetofauna between longitudes 26° and 136° E. The Himalaya, one of the world's most vulnerable regions to climate change, falls between these longitudes. In this context, there is a pressing need to better understand the effects of climate change on Himalayan amphibians.

One of the current approaches to quantifying the future distribution of species under climate change is the application of environmental niche models (ENMs). These models can provide information on the potential changes in species distributions (Thuiller et al., 2005), identify critical habitats and prioritize conservation areas (Heinrichs et al., 2010; DEPI, 2013), guide the management of invasive species (Jiménez-Valverde et al., 2011), help assess disease risk to biodiversity (Murray et al., 2011) or contribute to examinations of the efficacy of reserve systems (Araújo et al., 2004). However, under climate change one of the most implausible assumptions of conventional ENMs is that the species distribution is in equilibrium with climate, i.e., species will immediately react to the changing climate by shifting, expanding or contracting their ranges. This assumption is highly improbable, as it does not consider species' biotic responses and dispersal or migration constraints (Barve et al., 2011; Nobis and Normand, 2014), thus resulting in under- or overestimation of species distributions. Hence, the migrational ability of a species is a crucial factor for predicting its distribution under climate change. Most future ENM projections of species distributions still assume either unlimited or no migration, while the reality falls in between these two extremes (Pearson, 2006).

Nevertheless, there are methods available which enable species-specific dispersal and migration constraints in ENM projections. For instance, the MigClim model (Engler and Guisan, 2009) incorporates parameters such as species dispersal distance, barriers to dispersal and potential propagule production to obtain more realistic future species distributions compared with predictions from models that assume unlimited or no dispersal. To parameterize such models, a deep understanding of the ecology and life history of each single species is crucial. This information, however, is not available for most species, and dynamic models like MigClim that are built upon basic processes still assume a range of potential parametrization for their dispersal or demography components. In such cases, the KISSMig model (Nobis and Normand, 2014) is a useful alternative because it requires no assumptions about demography or dispersal/movement processes. Without simulating the underlying processes, KISSMig can be directly used for the evaluation of different migration rates, and it was proven successful in simulating species distributions under climate change scenarios (Nobis and Normand, 2014; Kissling et al., 2016).

To explore effects of climate change on the future distribution of amphibians in the Himalaya, we developed ENMs in combination with various migration scenarios for four species of high elevation frogs belonging to the genus *Scutiger*. This genus is found in high mountains and cold deserts across High Asia and is represented globally by 21 species (Hofmann et al., 2017). Nearly half of the species (43%) are in the threatened category (IUCN, 2016). We chose four *Scutiger* species as model systems based on (1) their varying range sizes and (2) the availability of sufficient and reliable occurrence records throughout their entire species range. The general aim of our study was to form a better understanding of varying migration constraints on the future distribution of high elevation amphibians under climate change.

In the current study, we set three major objectives:

a. To develop ENMs of four high elevation frogs with varying range sizes in the Himalaya for the current period and for three future periods under two contrasting climate change scenarios.
b. To use these models to simulate future species distributions without migration, with unlimited migration, and with three plausible migration scenarios to generate more realistic projections of future species distributions.
c. To assess the relevance of migration constraints and discuss implications for conservation of the four *Scutiger* species, as well as other high elevation amphibians in the Himalayan ecoregion.

2. Materials and methods

2.1. Current species ranges and choice of predictors

Our study species were four high elevation anurans belonging to the genus *Scutiger*, i.e., *S. boulengeri*, *S. tuberculatus*, *S. glandulatus* and *S. sikimmensis*. While *S. boulengeri* has a wide distribution in the Himalaya, the other three species have relatively narrow ranges (Fig. 1). *Scutiger boulengeri* is one of the frog species occurring at the highest elevations in the world; it is reported to be found up to 5490 m a.s.l. (Subba et al., 2015). We documented species occurrences during field surveys from 2013 to 2016 by recording GPS coordinates and elevation. The elevation of species occurrences in our records ranged from 2400 to 5500 m a.s.l. The species records were complemented by secondary data points from the Global Biodiversity Information Facility (GBIF, http://www.

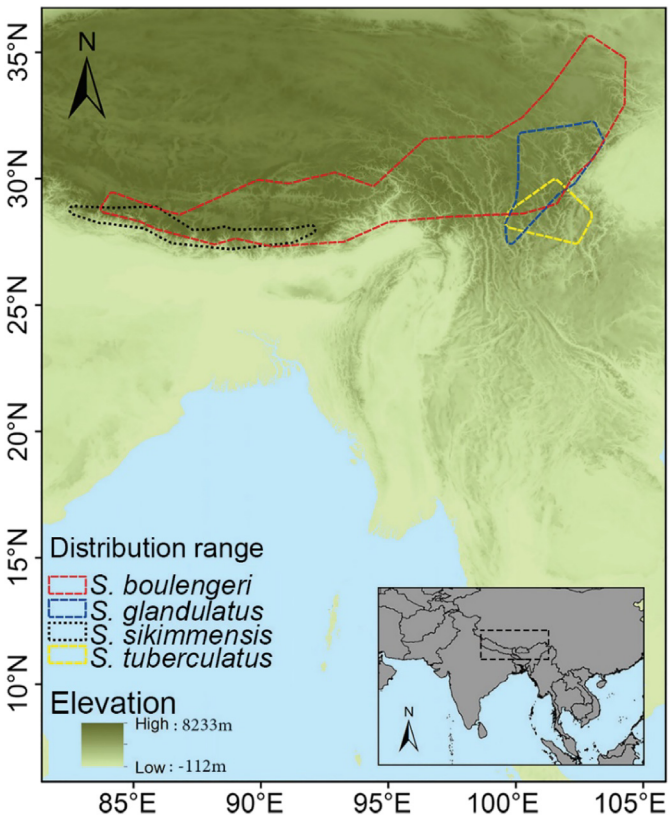

Fig. 1. Calculated species ranges of the four study species, *Scutiger boulengeri*, *S. glandulatus*, *S. sikimmensis* and *S. tuberculatus*. The map in the inset shows the location of the study area.

gbif.org/) and from literature (Fu et al., 2007; W. Chen et al., 2009). We chose 19 bioclimatic variables from the WorldClim dataset (Hijmans et al., 2005) averaged from 1960 to 1990 (hereafter referred to as current) and seven topographic and geographic variables that represent slope, aspect (northness and eastness) of the study area, hydrologically conditioned digital elevation models (DEM), stream flow, flow direction and flow accumulation (https://lta.cr.usgs.gov/HYDRO1K) to develop current ENMs. All the predictor layers had a spatial resolution of 1 km, 5 km and 10 km. Current species ranges were calculated based on the available species occurrence data by creating alpha-shapes using the *ashape* function implemented in the R package 'alphahull' (Pateiro-López and Rodrıguez-Casal, 2010), setting alpha to 2 and adding a buffer of 20 km (Fig. 1). More details about the occurrence data and species ranges are given in Appendix S1. A general overview of our modelling approach is provided in Appendix S2.

2.2. Niche modelling for the current period and for future scenarios

We used MaxEnt (Ver. 3.3.3; Phillips et al., 2006) for developing ENMs. The occurrence points were rarefied prior to model building to avoid the effect of spatial autocorrelation (Boria et al., 2014). The occurrences were rarefied at several graduated distances after calculating environmental heterogeneity of the study area using SDMToolbox (Brown, 2014). For developing the model, we used 57, 33, 23 and 11 rarefied occurrence points for *S. boulengeri*, *S. glandulatus*, *S. sikimmensis* and *S. tuberculatus*, respectively. To remove the effect of potential sampling bias, we created a bias grid by calculating a Gaussian kernel density map of the rarefied occurrence locations of all four species using SDMToolbox (Brown, 2014). The bias file was then used in MaxEnt to weight background points (Elith et al., 2010; Fourcade et al., 2014).

As collinear variables can influence the accuracy of species distribution models (Dormann et al., 2013), variables having a Pearson's correlation coefficient $|r| \geq 0.70$ were removed prior to model building, following Dormann et al. (2013). To avoid overfitting, we first developed a set of MaxEnt models with varying complexities for a range of regularization multipliers (0.5–2.5) and different feature type combinations (i.e., linear, product, quadratic, threshold and hinge). The R package 'ENMeval' (Muscarella et al., 2014) was used to tune and select the best current model based on 10-fold cross-validated omission rates and AUCcv, applying thresholds of the minimum training presence (MTP) (Table 1). To create binary maps of suitable and unsuitable areas, a 0.5 suitability threshold was used, following Liu et al. (2005).

To develop ENMs for future climates, we used climate scenarios for three future periods and averaged the data for the years 2021–2040, 2041–2060 and 2061–2080, hereafter referred to as 2040, 2060 and 2080, respectively. The layers were downloaded from the Research Program on Climate Change, Agriculture and Food Security of the Consultative Group on International Agricultural Research (CGIAR) web portal (ccafs-climate.org) for two climate change scenarios, RCP4.5 and RCP8.5, and at resolutions of 1 km, 5 km and 10 km. Furthermore, to explore the uncertainties associated with global circulation models (GCMs), we used three GCMs for each period, i.e., Hadley Coupled Model V3 (HadCM3_AO), Commonwealth Scientific and Industrial Research Organization (CSIRO_MK), and Beijing Climate Center Climate System Model (BCC-CSM1.1). In addition to using a 1 × 1 km standard resolution, the models were built using the same predictors with spatial resolutions of 5 × 5 km and 10 × 10 km.

Table 1
Summary of model evaluation statistics for the study species using ENMeval with varying model complexities. The features L, Q, P, T and H are the linear, quadratic, product, threshold and hinge features of MaxEnt, respectively. RM is the regularization multiplier value. OR is the 10-fold cross-validated omission rate, AUCcv is the 10-fold cross-validated AUC. ORmin is the minimum training presence omission rate and 10% OR is 10% of the omission rate.

Species	Predictor variables	MaxEnt features	RM	AUCcv	ORmin	10% OR
S. boulengeri	Bioclim 2,3,4,11,15,17 Flow accumulation	LQP	2	0.79	0.004	0.015
S. glandulatus	Bioclim 3,7,11,16,17 Flow accumulation	LQH	2	0.94	0.006	0.026
S. sikimmensis	Bioclim 3,11,15,19 Flow accumulation	LQPTH	2	0.88	0.000	0.13
S. tuberculatus	Bioclim 4,7,11,15,16,19 Flow accumulation	LQH	2	0.93	0.1	0.3

Table 2
Migration scenarios based on different numbers of iteration steps and the corresponding maximal migration rates per year (map resolutions: 1 km, 5 km and 10 km).

Simulated migration scenarios	Number of iteration steps per 20-year period			Maximal migration rates in km per year
	1 km	5 km	10 km	
MIG1	10	2	1	0.5
MIG2	50	10	5	2.5
MIG3	200	40	20	10

Table 3
List of predictors used for model building. Predictors chosen after a collinearity test are highlighted in bold.

Sl.	Predictor	Source
1	**BIO1 = annual mean temperature**	worldclim.org
2	**BIO2 = mean diurnal range (mean of monthly (max temp − min temp))**	worldclim.org
3	**BIO3 = isothermality (BIO2/BIO7) (∗100)**	worldclim.org
4	**BIO4 = temperature seasonality (standard deviation ∗100)**	worldclim.org
5	BIO5 = max temperature of warmest month	worldclim.org
6	BIO6 = min temperature of coldest month	worldclim.org
7	BIO7 = temperature annual range (BIO5-BIO6)	worldclim.org
8	BIO8 = mean temperature of wettest quarter	worldclim.org
9	BIO9 = mean temperature of driest quarter	worldclim.org
10	BIO10 = mean temperature of warmest quarter	worldclim.org
11	**BIO11 = mean temperature of coldest quarter**	worldclim.org
12	BIO12 = annual precipitation	worldclim.org
13	BIO13 = precipitation of wettest month	worldclim.org
14	BIO14 = precipitation of driest month	worldclim.org
15	**BIO15 = precipitation seasonality (coefficient of variation)**	worldclim.org
16	**BIO16 = precipitation of wettest quarter**	worldclim.org
17	**BIO17 = precipitation of driest quarter**	worldclim.org
18	BIO18 = precipitation of warmest quarter	worldclim.org
19	**BIO19 = precipitation of coldest quarter**	worldclim.org
20	Hydrologically conditioned DEM	lta.cr.usgs.gov/HYDRO1K
21	Stream flow	lta.cr.usgs.gov/HYDRO1K
22	Flow direction	lta.cr.usgs.gov/HYDRO1K
23	**Flow accumulation**	lta.cr.usgs.gov/HYDRO1K
24	Slope	Calculated from DEM
25	Aspect (northness)	Calculated from DEM
26	Aspect (eastness)	Calculated from DEM

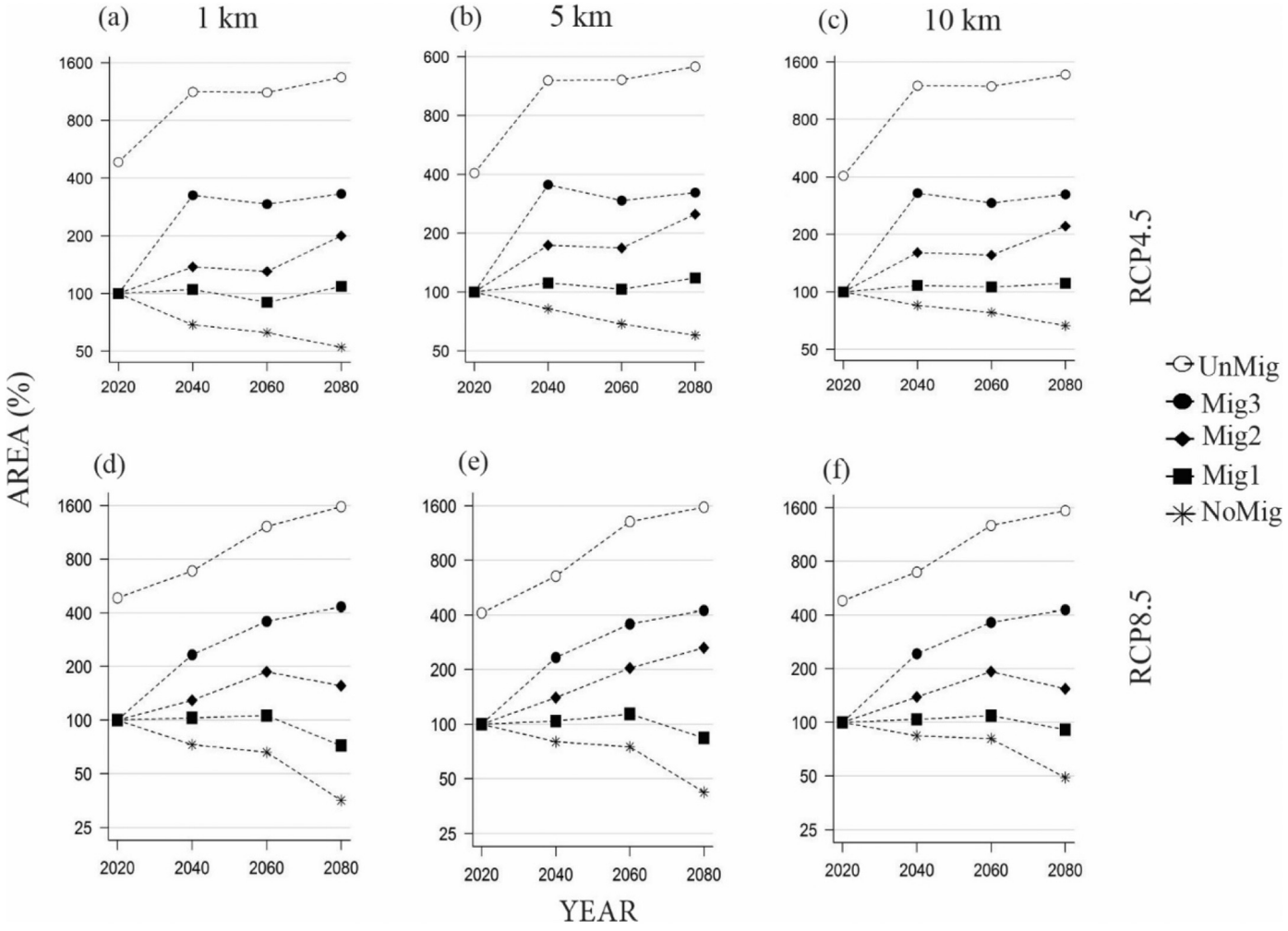

Fig. 2. Simulated dynamics of the distribution area with different maximal migration rates for *Scutiger sikimmensis*. (a), (b) and (c) correspond to RCP4.5 with a map resolution of 1 km, 5 km and 10 km, respectively; (d), (e) and (f) correspond to RCP8.5 with a map resolution of 1 km, 5 km and 10 km, respectively. UnMig = unlimited migration scenario. MIG1 = maximal migration rate of 0.5 km/yr. MIG2 = maximal migration rate of 2.5 km/yr. MIG3 = maximal migration rate of 10 km/yr. NoMig = no migration scenario. Y-axes are log-scaled.

2.3. Direct modelling of species migration

We used KISSMig (Nobis and Normand, 2014), a raster-based stochastic migration model, to generate future species distributions. Starting from an initial species distribution (current), KISSMig simulates distribution dynamics on top of suitability maps with a simple 3 × 3 cell algorithm. We used squared values of MaxEnt suitability for KISSMig simulations (http://purl.oclc.org/wsl/kissmig; kissmig_suitability.pdf). To evaluate the effects of varying migration constraints, we applied different maximal migration rates, i.e., different numbers of iteration steps applying the 3 × 3 cell algorithm. The number of iteration steps was adjusted across the models with different spatial resolutions to keep migration rates constant (Table 2). Based on a recent review on amphibian movement capacities (Sinsch, 1990), we considered “low”, “medium” and “high” migration scenarios that represent maximal migration rates of 0.5 km/y, 2.5 km/y, and 10 km/y, respectively. These migration scenarios are referred to hereafter as MIG1 (low), MIG2 (medium) and MIG3 (high).

For the migration simulations, the initial distribution of each species was calculated by (a) starting with all pixels of the current species range occupied by the species, (b) running KISSMig with a spin-up of 200 iteration steps and the current suitability map to restrict occupied cells to suitable areas, and (c) finally deleting all occupied cells outside the current species range. The future species dynamics were thereafter calculated using KISSMig calls using this initial species distribution along with the three future suitability maps as a raster stack and one of the migration rates (low, medium or high), i.e., numbers of iteration steps (Appendix S2).

3. Results

3.1. Model performance and general trends

Ten variables, including nine bioclimatic variables and one hydrological variable (flow accumulation), fulfilled the correlation requirements ($|r| < 0.70$) and were selected during model building (Table 3, Appendix S3). The MaxEnt models performed from fair to excellent (Araújo et al., 2005), with AUCcv values of 0.79, 0.88, 0.93 and 0.94 for *S. boulengeri*, *S. sikimmensis*, *S. tuberculatus* and *S. glandulatus*, respectively (Table 1). The future projections of suitable area under the three different GCMs were highly congruent for all the species, and therefore we averaged the results of each period under two RCPs. The no-migration scenarios for all the species consistently showed a decline (−15% to −64%) in suitable area by 2080 under both the RCP4.5 and the RCP8.5 scenario (Figs. 2, 3 and Appendices S3–S5). For all the study species, considerable differences were observed between the distribution area predicted by MaxEnt and future distributions under different plausible migration constraints (Figs. 2, 3 and Appendices S4–S6).

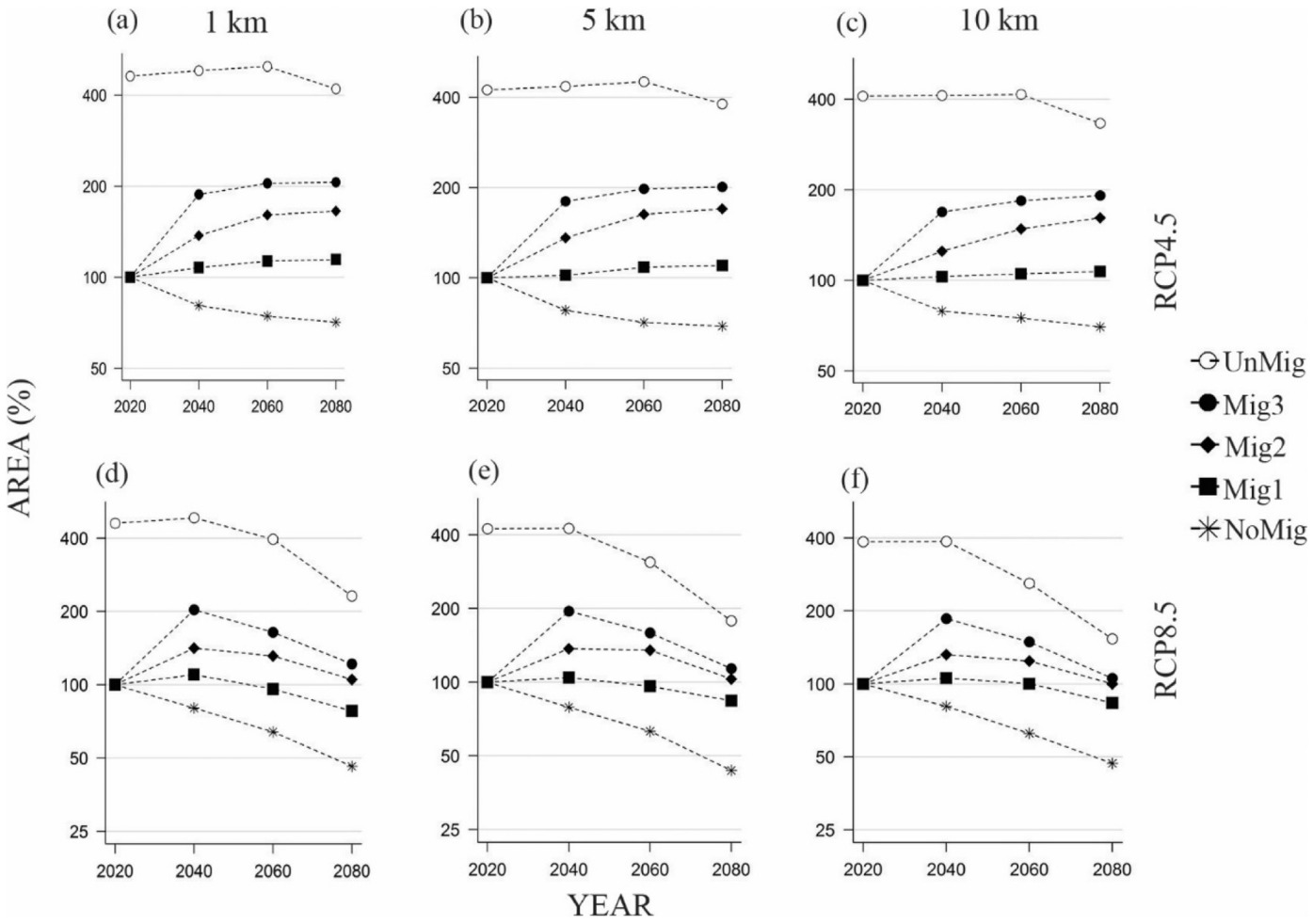

Fig. 3. Simulated dynamics of the distribution area with different maximal migration rates for *Scutiger tuberculatus*. (a), (b) and (c) correspond to RCP4.5 with a map resolution of 1 km, 5 km and 10 km, respectively; (d), (e) and (f) correspond to RCP8.5 with a map resolution of 1 km, 5 km and 10 km, respectively. UnMig = unlimited migration scenario. MIG1 = maximal migration rate of 0.5 km/yr. MIG2 = maximal migration rate of 2.5 km/yr. MIG3 = maximal migration rate of 10 km/yr. NoMig = no migration scenario. Y-axes are log-scaled.

Suitable areas for all species showed a northward and upward shift in future scenarios (Figs. 4, 5 and Appendices S6, S7). Correspondingly, most future distributions had the features of leading edges at higher latitudes or elevations, and tailing edges at lower latitudes or elevations (Fig. 5 and Appendix S6). In addition, the simulations revealed that most of the suitable area predicted under unlimited migration would remain uncolonized even if the species were to migrate at a high rate (Figs. 2, 3 and Appendices S5, S6).

3.2. Predicted changes in species distributions

3.2.1. Scutiger sikimmensis

The predicted suitable area for *S. sikimmensis* under current conditions covered c. 1,81,345 km^2, of which c. 35,488 km^2 overlapped with the current species range consisting of Sikkim (India), Bhutan, parts of western, central and eastern Nepal facing the Himalaya, and a small part of southern Xizang (China) (Fig. 4, Appendices S1, S4; for simplicity, the number of suitable pixels is given as approximate area in square kilometres). The two most important predictors for suitable area were isothermality (BIO3) and flow accumulation, with contributions of 60.4% and 20.5%, respectively (Appendix S3). Under unlimited migration, *S. sikimmensis* showed the greatest relative gain in suitable area by 2080 in both RCP8.5 (+204%) and RCP4.5 (+163%). By contrast, in the absence of migration the species showed the strongest relative decline in suitable area in both RCP4.5 (−48%) and RCP8.5 (−64%) by 2080 (Fig. 2 and Appendices S4–S6). The projected species distributions showed distinct dynamics under different migration constraints. Depending on the plausible migration scenario applied, the change in the projected species distribution in 2080 ranged from −23% (RCP 8.5, MIG1) to +332% (RCP 8.5, MIG3) compared to the suitable area of the current species range (Appendix S4). When low or medium migration rates were applied, *S. sikimmensis* experienced a significant range fragmentation under RCP8.5 from the current period to 2080, indicating a probable formation of eastern and western populations in the future (Fig. 5, Appendix S6). In addition, even with the high migration rate the species could not reach newly suitable areas predicted to emerge in the eastern part of the study area.

3.2.2. Scutiger boulengeri

For *S. boulengeri* the predicted suitable area under current conditions covered c. 4,68,693 km^2, of which c. 3,64,234 km^2 overlapped with the current species range consisting of Sikkim and Arunachal Pradesh in India, southern and eastern parts of Xizang, western Sichuan and southwestern Gansu in China, and northern parts of western, central and eastern Nepal (Appendices S1, S4 and S6). Temperature of the coldest quarter (BIO11) and mean diurnal range (BIO2) were the two most important predictors in the MaxEnt model for *S. boulengeri*, with contributions of 66.9% and 13.7%, respectively (Appendix 3). Of all four species, *S. boulengeri* showed the smallest decrease in suitable area in future no-migration scenarios, ranging from −28% (RCP4.5) to

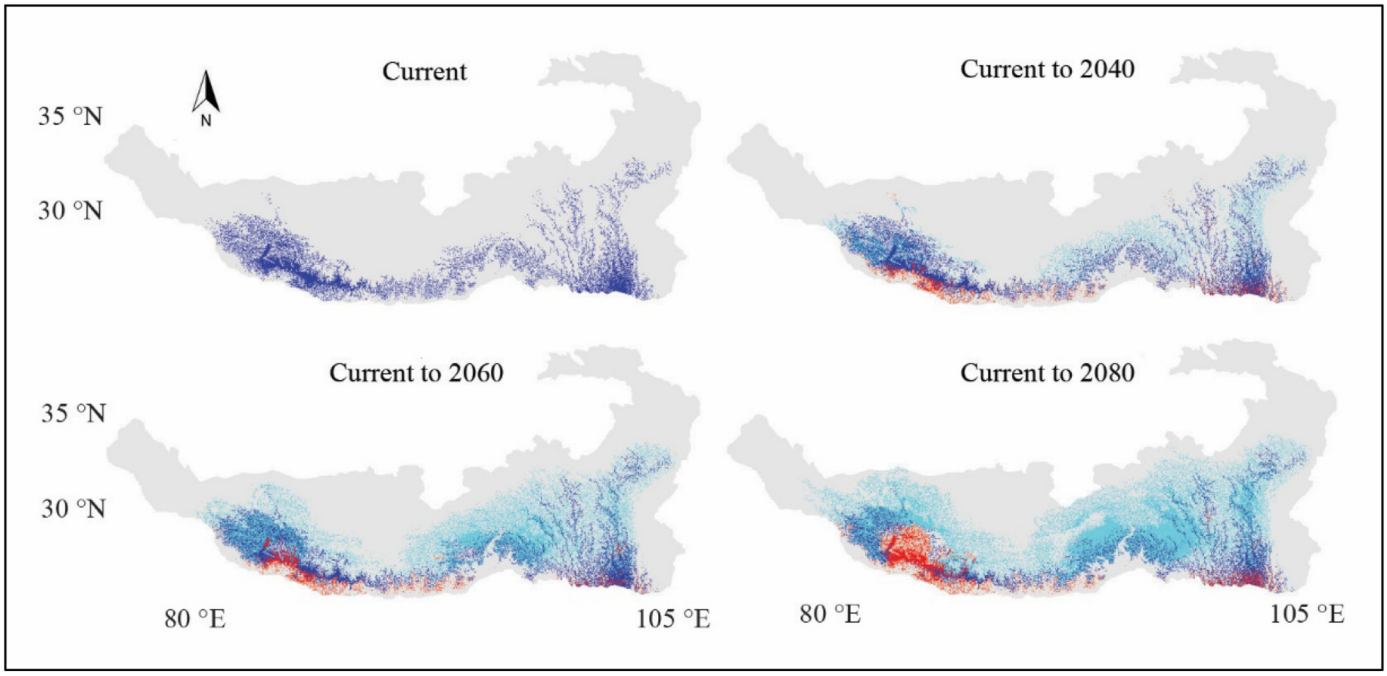

Fig. 4. Current and future suitability maps for *Scutiger sikimmensis* calculated with MaxEnt, RCP8.5 and 1 km spatial resolution. Colours represent future changes, with suitable areas becoming unsuitable shown in red, unsuitable areas becoming suitable in light blue, and areas remaining suitable in dark blue. (For interpretation of the references to colour in this figure legend, the reader is referred to the web version of this article.)

−42% (RCP8.5) by the year 2080 (Appendices S4–S6). Based on the different plausible migration scenarios, the change in the projected species distribution by 2080 ranged from a gain of +36% (RCP8.5, MIG1) to +109% (RCP8.5, MIG3) compared to the suitable area of the current species range (Appendix S4). The loss of future species distributions was most prominent in central and eastern Nepal, Sikkim (India), and the Sichuan and Gansu regions of China, whereas there was a gain in the northern and higher elevation regions of the current distribution under all three migration scenarios.

3.2.3. *Scutiger glandulatus*

The predicted suitable area for *S. glandulatus* under current conditions covered c. 1,45,332 km^2, of which c. 54,942 km^2 overlapped with the current species range consisting of parts of central Sichuan (Appendices S1, S4 and S6). The two most important predictors for habitat suitability of *S. glandulatus* were temperature of the coldest quarter (BIO11) and precipitation of the wettest quarter (BIO16), with contributions of 59.1% and 26.9%, respectively (Appendix S3). The species distribution under the no-migration scenario showed a maximal area loss of −50% by 2080 under RCP8.5 (Appendix S4). Under the plausible migration scenarios, the smallest gain in the distribution area by 2080 was +35% (RCP8.5, MIG1) and the largest gain was +389% (RCP4.5, MIG3) (Appendix S4). The three migration scenarios under RCP4.5 and RCP8.5 showed a loss of the species distribution in small parts of northern Yunnan and central-eastern Sichuan and a gain in the distribution area in northern and western Sichuan by 2080. Although suitable areas emerged in the Gansu, Qinghai and Xizang regions of China, Bhutan, Nepal and the north-eastern part of India, the species was not able to occupy these areas because of migration constraints and unsuitable migration barriers.

3.2.4. *Scutiger tuberculatus*

The predicted suitable area for *S. tuberculatus* under current conditions covered c. 2,06,584 km^2, of which c. 44,980 km^2 overlap with the current species range consisting of southern Sichuan (Appendices S1, S4 and S6). The two most important predictors for habitat suitability of *S. tuberculatus* were temperature of the coldest quarter (BIO11) and precipitation of the wettest quarter (BIO16), with contributions of 43.2% and 39.7%, respectively (Appendix S3). The unlimited migration scenario of MaxEnt suggested declines in suitable area of *S. tuberculatus* in future scenarios, with a loss of −10% and −50% by 2080 under RCP4.5 and RCP8.5, respectively. Under the no-migration scenario −33% (RCP4.5) and −53% (RCP8.5) of suitable area is predicted to be lost by 2080 (Appendix S4). Depending on the plausible migration scenario applied, the change in the species distribution by 2080 ranged from −22% (RCP8.5, MIG1) to +106% (RCP4.5, MIG3), compared to the suitable area of the current species range (Appendix S4). Interestingly, for all plausible migration rates the colonized area between 2040 and 2080 always increased under RCP4.5, but decreased under RCP8.5 (Fig. 3, Appendix S4).

4. Discussion

In this study, we combined widely used environmental niche models directly with different plausible migration scenarios to simulate more realistic species distributions under climate change. Below we discuss the strengths and limitations of our approach, as well as implications for conservation strategies.

Amphibians belonging to the genus *Scutiger* are expected to be vulnerable to climate change because of their relatively low dispersal capability, local endemism and adaptation to high elevations (Yiming and Cohen, 2013; Hofmann et al., 2017). According to MaxEnt, for all the four species, temperature was more important than precipitation or stream flow accumulation, and mean temperature of the coldest quarter (BIO11) was the most important predictor for three out of the four species (Appendix S3). Our findings also show that, in the absence of migration, all species are projected to lose parts of their current distribution. This loss is considered a good predictor of extinction risk (Koopowitz et al., 1994), and our results suggest that the study species are vulnerable to climate-induced threats. The general changes in suitable areas, as well as in projected distributions under limited migration, were consistent across models using different spatial resolutions (1 km, 5 km and 10 km), which demonstrates the robustness of our approach in this regard.

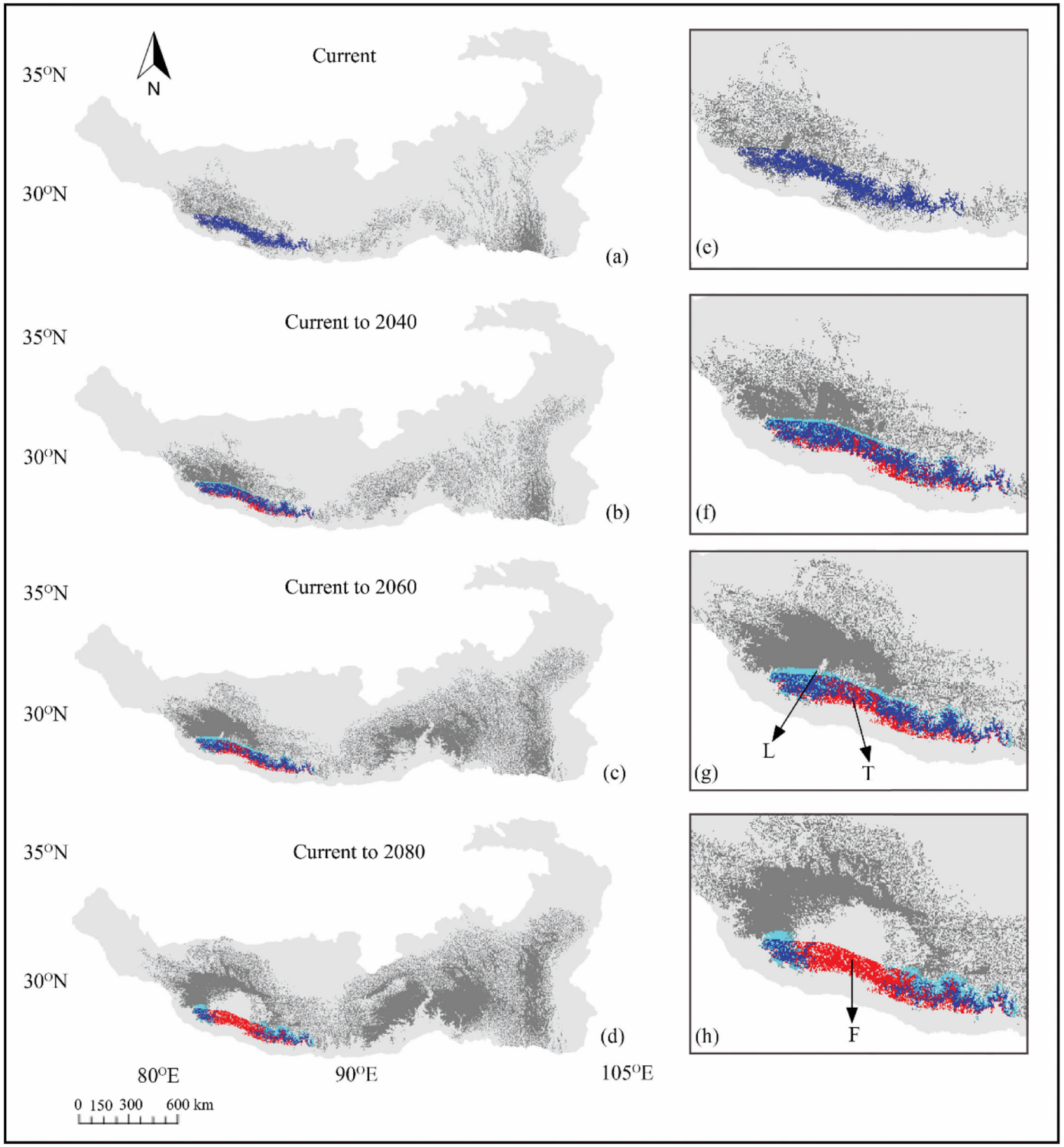

Fig. 5. Simulated current and future distribution maps for *Scutiger sikimmensis* calculated using KISSMig, MIG1, RCP8.5 and 1 km spatial resolution (a–d). Colours represent future changes, with suitable areas with no occurrences shown in dark grey, loss of distribution area or extinction in red, areas that are stable and remain colonized in dark blue and newly colonized areas through migration in light blue. The corresponding insets show the part of the study area, enclosed by a dashed rectangle in (a), and highlight leading and tailing/contracting edges and fragmentation of *Scutiger sikimmensis* into western and eastern populations (e–h). L = leading edge, T = tailing or contracting edge and F = fragmentation. (For interpretation of the references to colour in this figure legend, the reader is referred to the web version of this article.)

Unlimited migration models give a rather overoptimistic picture of species distributions in future climate change scenarios, whereas distribution models with plausible migration constraints give a more accurate view. For example, under unlimited migration, a gain of suitable area for *S. sikimmensis* was prominent in a very large region, covering most of the central, eastern and western Xizang (Tibetan plateau) region of China and northern parts of India, Nepal, Bhutan and Myanmar (Fig. 4 and Appendix S6). In comparison, the limited migration models showed precise and much smaller areas that could possibly be colonized by the species (Fig. 5 and Appendix S6). These results indicate that such

species might access only a very small fraction of the projected suitable area, even under contrasting migration scenarios. These differences in suitable and accessible areas between correlative and dynamic distribution models demonstrate the importance of incorporating migration constraints into future projections of species distributions.

The direct combination of common ENMs with migration scenarios also resulted in more realistic detection of stable versus dynamic areas with leading and tailing edges. Such spatially explicit information is crucial for strategies and action plans in nature conservation. Stable areas predicted in the absence of migration might contain the most viable populations and can act as future refugia. Additional areas predicted under low migration rates are the most likely locations to be newly colonized in the future and might represent important migration corridors for a species to track climate change. As the species moves towards higher latitudes in the future, the populations at leading edges will likely prosper, whereas there will probably be a reduction in population size at the tailing edges, with an increasing probability of local extinctions. We propose that areas accessible under medium plausible migration rates should be considered for ensuring sequential connectivity between present and future ranges. In addition, our results suggest that some species ranges will become fragmented in the future (Fig. 5), which could have detrimental effects on species persistence. Habitat loss and fragmentation are the largest threat to amphibians (Becker et al., 2007); thus, these changes in species distributions may further threaten the genetic connectivity of populations (Allentoft and O'Brien, 2010).

Our study also demonstrates that even if a species is able to migrate at high rates, it still will not be able to track the majority of areas predicted under unlimited migration. On the other hand, highly suitable areas that are only accessible under unrealistically high migration rates should be considered further for assisted migration or ex situ conservation purposes (Ladle and Whittaker, 2011).

Our findings are important for conservation because many prioritization schemes still incorporate niche models that do not account for migration and may therefore produce unrealistic results (Bateman et al., 2013). This practice can heavily bias conservation plans by leading to the investment of resources into areas that might not be accessible by species because of their inherent dispersal limitations. Thus, conservation strategies may benefit from both species-specific and site-specific action plans.

We acknowledge that there are uncertainties associated with our approach. For example, our models do not account for complex interactions with other drivers of species dynamics, like habitat degradation, land-use changes or disease spread. Furthermore, the robustness of results using different modelling techniques was not evaluated because we focused on including spatially explicit migration and evaluating its general relevance in the context of high elevation amphibians. Another issue that is common in dynamic distribution models is the initial species distribution. We used all cells of a given species range colonized after an initial KISSMig run, which restricts the initial distribution to suitable areas (model 'spin up', as in Nobis and Normand, 2014). KISSMig simulations, nevertheless, showed an increase in occupied area, particularly for the first time-step until 2040, which might be partly because detailed contemporary species distributions were not available and range maps were used instead. This point applies especially to *S. tuberculatus*, which had the lowest number of occurrences available for building the range map. In some simulations of the first time-step until 2040, this species showed an unrealistic spread in all directions that vanished in later periods (Appendix S6).

5. Conclusions

In conclusion, even though ENMs have previously been proven to be useful for estimating the impact of global climate change on species distributions, incorporating species migration is important for achieving more realistic distribution dynamics and spatially explicit results. Different migration rates are useful for general comparison, while more information on the migration abilities of species is urgently needed. This would allow one to apply dynamic models that include dispersal kernels and demography on a more regular basis. As long as such information is not available for most species, the combination of simple migration models with common ENMs can provide helpful insights into the spatial dynamics and threats of species under environmental change.

Acknowledgements

B·S and S.S. benefitted from a Teaching Workshop for Niche Modelling 2016 held in Bangalore, India by Colorado State University in collaboration with National Centre for Biological Studies and Centre for Ecological Sciences. The manuscript was conceptualized during this workshop. We also thank Melissa Dawes for proof-reading the article and providing helpful comments. B.S. was supported from a grant from Critical Ecosystem Partnership Fund and Madras Crocodile Bank Trust for this project.

Appendix A. Supplementary data

Supplementary data to this article can be found online at https://doi.org/10.1016/j.biocon.2018.09.035.

References

Allentoft, M.E., O'Brien, J., 2010. Global amphibian declines, loss of genetic diversity and fitness: a review. Diversity 2, 47–71.
Araújo, M.B., Cabeza, M., Thuiller, W., Hannah, L., Willians, P.H., 2004. Would climate change drive species out of reserves? An assessment of existing reserve-selection methods. Glob. Chang. Biol. 10, 1618–1626.
Araújo, M.B., Pearson, R.G., Thuiller, W., Erhard, M., 2005. Validation of species–climate impact models under climate change. Glob. Chang. Biol. 11, 15041513.
Barnosky, A.D., Matzke, N., Tomiya, S., Wogan, G.O., Swartz, B., Quental, T.B., Marshall, C., McGuire, J.L., Lindsey, E.L., Maguire, K.C., Mersey, B., 2011. Has the Earth's sixth mass extinction already arrived? Nature 471, 51–57.
Barve, N., Barve, V., Jiménez-Valverde, A., Lira-Noriega, A., Maher, S.P., Peterson, A.T., Soberón, J., Villalobos, F., 2011. The crucial role of the accessible area in ecological niche modeling and species distribution modeling. Ecol. Model. 222, 1810–1819.
Bateman, B.L., Murphy, H.T., Reside, A.E., Mokany, K., VanDerWal, J., 2013. Appropriateness of full-, partial-and no-dispersal scenarios in climate change impact modelling. Divers. Distrib. 19, 1224–1234.
Becker, C.G., Fonseca, C.R., Haddad, C.F.B., Batista, R.F., Prado, P.I., 2007. Habitat split and the global decline of amphibians. Science 318, 1775–1777.
Bishop, P.J., Angulo, A., Lewis, J.P., Moore, R.D., Rabb, G.B., Moreno, G., 2012. The amphibian extinction crisis – what will it take to put the action into the amphibian conservation action plan? Sapiens 5, 1–15.
Boria, R.A., Olson, L.E., Goodman, S.M., Anderson, R.A., 2014. Spatial filtering to reduce sampling bias can improve the performance of ecological niche models. Ecol. Model. 275, 73–77.
Brown, J.L., 2014. SDMtoolbox: a python-based GIS toolkit for landscape genetic, biogeographic and species distribution model analyses. Methods Ecol. Evol. 5, 694–700.
Chen, F., Wang, J., Jin, L., Zhang, Q., Li, J., Chen, J., 2009. Rapid warming in mid-latitude central Asia for the past 100 years. Front. Earth Sci. 3, 42–50.
Chen, W., Bi, K., Fu, J., 2009. Frequent mitochondrial gene introgression among high elevation Tibetan megophryid frogs revealed by conflicting gene genealogies. Mol. Ecol. 18, 2856–2876.
DEPI, 2013. Biodiversity Information Tools for Use in Native Vegetation Decisions. The State of Victoria Department of Environment and Primary Industries, Department of Environment and Primary Industries, Melbourne, Australia.
Dormann, C.F., Elith, J., Bacher, S., Buchmann, C., Carl, G., Carré, G., Marquéz, J.R.G., Gruber, B., Lafourcade, B., Leitão, P.J., Münkemüller, T., 2013. Collinearity: a review of methods to deal with it and a simulation study evaluating their performance. Ecography 36, 27–46.
Elith, J., Kearney, M., Phillips, S., 2010. The art of modelling range-shifting species. Methods Ecol. Evol. 1, 330–342.
Engler, R., Guisan, A., 2009. MigClim: predicting plant distribution and dispersal in a changing climate. Divers. Distrib. 15, 590–601.
Fourcade, Y., Engler, J.O., Rödder, D., Secondi, J., 2014. Mapping species distributions with MAXENT using a geographically biased sample of presence data: a performance assessment of methods for correcting sampling bias. PLoS One 9, e97122. https://doi.org/10.1371/journal.pone.0097122.
Fu, J., Weadick, C.J., Bi, K., 2007. A phylogeny of the high-elevation Tibetan megophryid frogs and evidence for the multiple origins of reversed sexual size dimorphism. J. Zool. 273, 315–325.
Heinrichs, J.A., Bender, D.J., Gummer, D.L., Schumaker, N.H., 2010. Assessing critical

habitat: evaluating the relative contribution of habitats to population persistence. Biol. Conserv. 143, 2229–2237.
Hijmans, R.J., Cameron, S.E., Parra, J.L., Jones, P.G., Jarvis, A., 2005. Very high resolution interpolated climate surfaces for global land areas. Int. J. Climatol. 25, 1965–1978.
Hofmann, S., Stöck, M., Zheng, Y., Ficetola, F.G., Li, J.T., Scheidt, U., Schmidt, J., 2017. Molecular phylogenies indicate a paleo-Tibetan origin of Himalayan lazy toads (*Scutiger*). Sci. Rep. 7.
IPCC, 2013. Climate Change 2013: The physical science basis. In: Stocker, T.F., Quin, D., Plattner, G.K., Tignor, M., Allen, S.K., Boschung, J., Nauels, A., Xia, Y., Bex, V., Midgley, P.M. (Eds.), Contribution of Working Group I to the Fifth Assessment Report of the Intergovernmental Panel on Climate Change. Cambridge University Press, Cambridge, United Kingdom and New York, NY, USA, pp. 1535.
IUCN, 2016. International Union for Conservation of Nature red list. http://www.iucn.org/about/work/programmes/species/red_list/.
Jiménez-Valverde, A., Peterson, A.T., Soberón, J., Overton, J.M., Aragón, P., Lobo, J.M., 2011. Use of niche models in invasive species risk assessments. Biol. Invasions 13, 2785–2797.
Kissling, W.D., Blach-Overgaard, A., Zwaan, R.E., Wagner, P., 2016. Historical colonization and dispersal limitation supplement climate and topography in shaping species richness of African lizards (Reptilia: Agaminae). Sci. Rep. 6.
Koopowitz, H., Thornhill, A.D., Andersen, M., 1994. A general stochastic model for the prediction of biodiversity losses based on habitat conversion. Conserv. Biol. 8, 425–438.
Ladle, R., Whittaker, R.J. (Eds.), 2011. Conservation Biogeography. John Wiley & Sons.
Lawler, J.J., Shafer, S.L., White, D., Kareive, P., Maurer, E.P., Balustein, A.R., Bartlein, P.J., 2009. Projected climate induced faunal change in the Western Hemisphere. Ecology 90, 588–597.
Leadley, P., 2010. Biodiversity Scenarios: Projections of 21st Century Change in Biodiversity, and Associated Ecosystem Services: A Technical Report for the Global Biodiversity Outlook 3 (No. 50). UNEP/Earthprint.
Leung, B., Greenberg, D.A., Green, D.M., 2017. Trends in mean growth and stability in temperate vertebrate populations. Divers. Distrib. 23, 1372–1380.
Li, Y., Zhai, S.N., Qiu, Y.X., Guo, Y.P., Ge, X.J., Comes, H.P., 2011. Glacial survival east and west of the 'Mekong–Salween Divide' in the Himalaya–Hengduan Mountains region as revealed by AFLPs and cpDNA sequence variation in *Sinopodophyllum hexandrum* (Berberidaceae). Mol. Phylogenet. Evol. 59, 412–424.
Li, J., McCarthy, T.M., Wang, H., Weckworth, B.V., Schaller, G.B., Mishra, C., Beissinger, S.R., 2016. Climate refugia of snow leopards in High Asia. Biol. Conserv. 203, 188–196.
Liu, C., Berry, P.M., Dawson, T.P., Pearson, R.G., 2005. Selecting thresholds of occurrence in the prediction of species distributions. Ecography 28, 385–393.
Murray, K.A., Retallick, R.W., Puschendorf, R., Skerratt, L.F., Rosauer, D., McCallum, H.I., VanDerWal, J., 2011. Assessing spatial patterns of disease risk to biodiversity: implications for the management of the amphibian pathogen, *Batrachochytrium dendrobatidis*. J. Appl. Ecol. 48, 163–173.
Muscarella, R., Galante, P.J., Soley-Guardia, M., Boria, R.A., Kass, J.M., Uriarte, M., Anderson, R.P., 2014. ENMeval: an R package for conducting spatially independent evaluations and estimating optimal model complexity for Maxent ecological niche models. Methods Ecol. Evol. 5, 1198–1205.
Nobis, M.P., Normand, S., 2014. KISSMig – a simple model for R to account for limited migration in analyses of species distributions. Ecography 37, 1282–1287.
Pateiro-López, B., Rodrıguez-Casal, A., 2010. Generalizing the convex hull of a sample: the R package alphahull. J. Stat. Softw. 34, 1–28.
Pearson, R.G., 2006. Climate change and the migration capacity of species. Trends Ecol. Evol. 21, 111–113.
Phillips, S.J., Anderson, R.P., Schapire, R.E., 2006. Maximum entropy modeling of species geographic distributions. Ecol. Model. 190, 231–259.
Sala, O.E., Chapin, F.S., Armesto, J.J., Berlow, E., Bloomfield, J., Dirzo, R., Huber-Sanwald, E., Huenneke, L.F., Jackson, R.B., Kinzig, A., Leemans, R., 2000. Global biodiversity scenarios for the year 2100. Science 287, 1770–1774.
Shrestha, U.B., Bawa, K.S., 2014. Impact of climate change on potential distribution of Chinese caterpillar fungus (*Ophiocordyceps sinensis*) in Nepal Himalaya. PLoS One 9, e106405. https://doi.org/10.1371/journal.pone.0106405.
Sinsch, U., 1990. Migration and orientation in anuran amphibians. Ethol. Ecol. Evol. 2, 65–79.
Subba, B., Ravikanth, G., Aravind, N.A., 2015. Scaling new heights: first record of Boulenger's Lazy Toad *Scutiger boulengeri* (Amphibia: Anura: Megophryidae) from high altitude lake in Sikkim Himalaya, India. J. Threat. Taxa 107, 655–7663.
Telwala, Y., Brook, B.W., Manish, K., Pandit, M.K., 2013. Climate-induced elevational range shifts and increase in plant species richness in a Himalayan biodiversity epicentre. PLoS One 8, e57103. https://doi.org/10.1371/journal.pone.0057103.
Thuiller, W., Lavorel, S., Araújo, M.B., Sykes, M.T., Prentice, I.C., 2005. Climate change threats to plant diversity in Europe. Proc. Natl. Acad. Sci. U. S. A. 102, 8245–8250.
Warren, R., VanDerWal, J., Price, J., Welbergen, J.A., Atkinson, I., Ramirez-Villegas, J., Lowe, J., 2013. Quantifying the benefit of early climate change mitigation in avoiding biodiversity loss. Nat. Clim. Chang. 3, 678–682.
Winter, M., Fiedler, W., Hochachka, W.M., Koehncke, A., Meiri, S., De la Riva, I., 2016. Patterns and biases in climate change research on amphibians and reptiles: a systematic review. R. Soc. Open Sci. 3, 160158.
WWF, 2015. Details available at. http://wwf.panda.org/, Accessed date: 3 February 2017.
Xu, J., Grumbine, R.E., Shrestha, A., Eriksson, M., Yang, X., Wang, Y.U.N., Wilkes, A., 2009. The melting Himalayas: cascading effects of climate change on water, biodiversity, and livelihoods. Conserv. Biol. 23, 520–530.
Yiming, L.I., Cohen, J.M., 2013. Review and synthesis of the effects of climate change on amphibians. Integr. Zool. 8, 145–161.